Antiviral Functionalization of a Polypropylene Nonwoven as Self Decontaminating Layer for Respiratory Masks

Mickael Maton, Sarah Gabut, Christel Neut, Pascal Odou, Camille Sacareau, Anthony Pinon, Michele Vialette, Gaetan Gerber, Bernard Martel, Nicolas Blanchemain

Antiviral Functionalization of a Polypropylene Nonwoven as Self Decontaminating Layer for Respiratory Masks

Mickael Maton[a], Sarah Gabut[a,b], Christel Neut[c], Pascal Odou[d], Camille Sacareau[e], Anthony Pinon[e], Michèle Vialette[e], Gaétan Gerber[f], Bernard Martel[b]*, Nicolas Blanchemain[a]*

The aim of this work was to develop a filtering biocidal PP nonwoven textile structure to block and inactivate airborne bacteria and viruses. PP filters were first functionalized with a cyclodextrin (CD)-polycarboxylic acid crosslinked polymer (PP-CD) through a pad/dry/curing process, and were then activated by padding in an alkyl dimethyl benzalkonium chloride (ADBAC) solution. The textile finishing process parameters were optimized with the perspective of mass production considering on one hand the threshold temperature necessary for provoking crosslinking and the limitation of the low thermal stability of PP on the other hand. The use an aqueous solution containing hydroxypropyl-β-cyclodextin (HPβCD), 1,2,3,4-butanetetracarboxylic acid (BTCA), ammonium hypophosphite (AH) and a surfactant allowed to immobilize the optimal quantity of cyclodextin polymer under curing at 125°C during 5 minutes without affecting the nonwoven PP structure. Presence of CD drastically increased the sorption of ADBAC on the textiles. Rinsing cycles evidenced ADBAC leaching at the first rinsing and good fastness at second and third rinsings, revealing adsorption mechanisms by weak physical interactions, ionic interactions and inclusion of ADBAC inside CD cavities. SEM study did not display any clogging of the nonwoven porosity neither any increase of air flow resistance evaluated by pressure drop measurements. Filtration efficiency of particulate matter $PM_{3.0}$ and $PM_{0.5}$ was moderately affected on contrary of $PM_{0.3}$ due to the loss of the electrosatic charge of the filter upon the functionalization process. Bactericidal tests displayed a reduction of 3 Log_{10} against *S. aureus* and virucidal tests on human coronavirus HCoV-229E displayed a reduction of 3.4 Log_{10} after 20 minutes of contact for both types of strains. Finally, the filter developped here is manufacturable by scalable process and displays filtration and biocidal performances that make of it a choice material as self-disinfecting layer in the fabrication of facepiece respirators.

1. Introduction

The world pandemic of COVID-19 has provoked the exponential demand for respiratory and surgical masks already used by health-care workers and currently adopted by the mainstream population as the first measures to limit the spread of SARS-CoV-2, the virus that causes COVID-19. At the beginning of the pandemic, the incidence of COVID-19 was significantly lower in countries where the mask was worn (129 cases per million) compared to countries that delayed adoption of the mask (> 1000 cases per million)[1]. Surgical masks avoid the spread by an infected person of the pathogens carried by droplets produced by breathing, talking, coughing or sneezing, while facemasks or respirators are considered as personal protective equipment that also protect the healthy wearer from inhaling airborne pathogens. After use life (recommended 4 hours), masks accumulate the filtered off viruses and present risks not only for the wearer himself, but may also provoke cross-contamination toward any third person that would subsequently be in contact with it[2].

[a] *Univ. Lille, INSERM, CHU Lille, U1008 – Advanced Drug Delivery Systems, Lille, France*
[b] *Univ. Lille, CNRS, INRAE, ENSCL UMR 8207, UMET – Unité Matériaux et Transformations, Lille, France*
[c] *Univ. Lille, INSERM, CHU Lille, U1286, Institute for Translational Research in Inflammation, Lille, France*
[d] *Univ. Lille, CHU Lille, ULR 7365 - GRITA - Groupe de Recherche sur les formes Injectables et les Technologies Associées, F-59000 Lille, France*
[e] *Institut Pasteur de Lille, Unité de Sécurité Microbiologique, 1 rue du Professeur Calmette, Lille, France*
[f] *Bioserenity, 47 bd de l'Hôpital, Paris, France*
Electronic Supplementary Information (ESI) available: [details of any supplementary information available should be included here]. See DOI: 10.1039/x0xx00000x

Therefore, the COVID-19 pandemic has spurred materials researchers to develop antiviral masks so that they do not just trap the coronavirus, but also destroys it. Self-decontaminating masks are produced by combining filtering structures with virucidal compounds such as natural viral inhibitors such as *Isatis indigotica*[3], metal or metal oxide nanoparticles (silver, copper, zinc), or organic substances (Polyphenol, PEI, N-halamines)[4]. Some were commercialized like HEIQ Viroblock® and Viral Off® (silver), Livingard® (polycationic surface), Sonovia® (zinc oxide), Wise Protect® and G-Fab® (quaternary ammonium salts). For their certification, French health authorities consider the intrinsic toxicity of the active molecule combined with the mask and the safety through the risk of diffusion to hands, face skin and mouth, and inhalation through the respiratory tract.

The anti-infective agents (AIA) like antimicrobial polymers, antibiotics, metal nanoparticles and metal oxides, natural compounds, quaternary ammonium, etc. must be securely bound to the textile substrate. Therefore, many strategies for textile finishing with AIA have been reported, adapted to each AIA afore mentioned[5]. Strategies such as atom transfer radical polymerization[6], coating with chitosan[7], spinning from molten PP compounded with silver or graphen[8,9], silver nanoclusters/silica composite[10], layer-by-layer deposition of bactericidal polymers[11], plasma activation[12], ultraviolet (UV)-initiated grafting[13], dip coating of a photopolymerisable active agent[14]; have been used.

Antiseptic properties of quaternary ammonium compounds (QACs) are known since a long time[15,16]. These synthetic compounds display broad-spectrum antimicrobial properties and present widespread applications such as components in cosmetic formulations, as germicides or softeners, bio-based

ionic liquids, catalysts in asymmetric catalysis, competitive inhibitors of acetylcholinesterase and nicotinic receptors[17]. In particular alkyl (C12, C14, C16) dimethyl benzyl ammonium chloride (ADBAC) that belong to the class of QACs have been used as active ingredients for their preservative properties of drug formulations for at least 50 years. In USA, ADBAC is approved as active ingredient by the Federal Food, Drug and Cosmetic Act (FFDCA) while it is regulated as a biocide under the Biocidal Products Regulation (BPR; Regulation (EU) 528/2012) administered by the European Chemicals Agency (ECHA) in Europe[18]. The biocidal activity of QACs stems from their cationic character combined with at least one long alkyl chain comprising 8 to 18 carbons. They strongly interact with the negative net charge present in the cell walls and membranes causing their clustering, ruptures and leakages. In particular, Dolezal et al. reported that alkyl chains of QACs composed of 12 to 16 carbons present the optimal antimicrobial activity[19]. QACs include broad-spectrum antimicrobial properties against Gram-negative and Gram-positive bacteria[20,21] and also against enveloped viruses such as SARS-Cov-2[22-24]. The antiviral activity of textile products is evaluated by tests according to the ISO18184 standard that measures the viral log reduction (or percent reduction) of the viral suspension in function of contact time with the bioactive textile

Cyclodextrins (CDs) are ring-shaped compounds obtained from starch enzymatic degradation, made of 6, 7, or 8 glucose repeat units called respectively α, β, and γ-cyclodextrins (α, β, γ-CDs), which present a central hydrophobic cavity that assign them the property of forming inclusion complexes with a wide range of organic compounds containing long alkyl chains or aromatic groups[25]. Since the early 2000s our groups have widely reported the use of textiles modified with cyclodextrins to immobilize and prolong the release of drugs like antibiotics[26], Silver[27], chlorhexidine[28], triclosan[29], or methylene blue[30]. Interestingly, Loftsson et al. have reported the formation of inclusion complex between CDs and organic salts such as ADBAC[31].

In 1999, we have proposed a chemical pathway that enabled the functionalization of chemically inert synthetic fibers by using a polycarboxylic acid as crosslinking agent. Interestingly, this process allowed the functionalization of chemically inert synthetic fibers such as polyethyleneterephtalate (PET)[32] then extended to polyamide[33], polylactic acid[34] and polypropylene[35]. The aim of this work was to develop a biocidal PP nonwoven structure capable of intercepting infected aerosols and droplets and inactivate them afterwards[36,37]. In a second phase, this biocide layer will be designated to be incorporated as a layer component of a respiratory mask. Therefore, the functional specifications of this biocide layer should obey both to filtration performances and to anti-pathogenic activity, or to the optimal compromise between these parameters.

In this study, the strategy was firstly to functionalize a polypropylene nonwoven with CD with polycarboxylic acid as crosslinking agent and a catalyst. The pad/dry/cure process parameters were optimized in order to preserve the textile structure (Filtration efficiency and air permeability) and from thermal degradation and to comply with industrial technical and economic requirements. Biocidal properties were then realized by loading ADBAC on the treated nonwoven. Finally, bactericidal (S. aureus and E. coli) and virucidal (HCoV-229E) tests were performed to evaluate the activity of this innovative biocidal PP non-woven textile.

2. Materials and Methods

2.1. Materials and chemicals

The textile filter used (MS50) was provided by Lydall (Melran, France). It consisted bilayered non-woven polypropylene (PP) textile fabricated by heat-welding followed by an electrostatic charge treatment. One side of MS50 was made of a spunbond layer (20 g/m²) and the other side was made of a meltblown layer (30 g/m²) so that the total surface weight was 50 g/m². Hydroxypropyl-β-cyclodextrin (HPβCD, Kleptose HP®, molar substitution MS = 0.85) was provided by Roquette (Lestrem, France). Citric acid monohydrate (CTR, ≥ 99.5%), sodium hypophosphite monohydrate ($NH_4H_2PO_2 \cdot H_2O$, ≥ 96%), 1-2-3-4 butanetetracarboxylic acid (BTCA, ≥ 99%), were purchased by Sigma Aldrich Chimie (Saint-Quentin Fallavier, France). Quaternary ammonium compounds, benzyl-C12-16-alkyldimethyl, chlorides (ADBAC) solution in water (50 % w/v) were purchased from mon-droguiste.com. Non-ionic surfactant (Erkantol®, Bayer, France) was added as auxiliary agent in the formulation for enhancing the wet pick-up of the reacting solution in the padding step.

2.2. Methods

2.2.1. Nonwoven finishing with cyclodextrin process

The pad-dry-cure process was applied using a roll-padder and a ventilated thermo fixation oven (Minithermo®) both from Roaches company (Leeds, GB). The non-woven sample (15 cm x 5 cm) was impregnated by padding in aqueous solutions containing 1) a polycarboxylic acid (BTCA or CTR), 2) a catalyst (sodium or ammonium hypophosphite), 3) a cyclodextrin (HPβCD) and 4) the surfactant (Erkantol®). The composition of the aqueous solution was reported as X/Y/Z/S, where X, Y, Z and S are related to the weight in gram unit of PCA, catalyst, CD and surfactant, respectively, dissolved in 100 mL of distilled water.

The impregnated textile was then roll-padded with a pressure of 2 bars at 1 meter per minute. A drying step at 90°C during 5 minutes was applied in the thermofixation oven, followed by a curing step between 120°C and 130 °C during 2 to 30 minutes to provoke the crosslinking reaction by esterification of HPβCD hydroxyls with BTCA or CTR carboxylic acid groups[38]. The PP nonwoven coated with CD polymer (PP-CD) was then roll padded with a pressure of 2 bars at 1 meter per minute in aqueous solutions of ADBAC, of concentrations 0.2% w/v, 0.5% w/v and 1.0% w/v, and dried in the thermofixation oven at 100 °C (PP-CD-0.2%; PP-CD-0.5% and PP-CD-1.0%).

After treatment, the degree of functionalization was measured by the weight gain of the fabric. Aliquots of 100 cm² disks were cut off from treated nonwoven rolls with a standard punch of 100 cm² purchased from Verson Vlies Coursier, (Linselles, France). Disk samples were washed with distilled water at ambient temperature with hand gentle agitation during 60 seconds and dried at 104 °C during 30 minutes and cooled in a desiccator during 15 minutes before weighing. The weight gain of the samples was calculated from the equation:

$$Weight\ Gain\ \% = \frac{m_f - m_i}{m_f} \text{ x } 100$$

where m_i and m_f are respectively the weight of 100 cm² aliquot sample before and after treatment measured with a precision balance (Kern, Germany).

2.2.2. SEM observation

The morphological architectures of MS50 before and after the finishing process were observed using scanning electron microscopy (SEM) (Hitachi SS 4700 SEM field emission GU) with an accelerating voltage of 5 kV and an emission current of 10 µA. All specimens were sputtered with a thin layer of chrome before imaging.

2.2.3. Filtration efficiency and air permeability

An airborne particles counter (AeroTrak® model 9550) was used for the characterization of air filtration performances of the nonwoven mats. The flow rate was fixed at 50 L/min (1.77 CFM) and count bin sizes ranged from 0.3 to 3 µm. This test was performed according to NF EN 14683: Requirements and test methods for masks for medical use (august 2019).

For filtration efficiency tests, textile samples were placed on the isokinetic probe (diameter 6 cm) of the particle counter and submitted to air flow of 50 L per hour. The filtration efficiency (η, %) could be obtained according to the following equation[39]

$$\eta = 1 - \frac{C_{downstream}}{C_{upstream}} x100$$

where $C_{downstream}$ and $C_{upstream}$ are the particle concentrations downstream and upstream, respectively.

The filtration efficiency toward particulate maters of 0.3 µm, 0.5 µm and 3 µm was measured ($PM_{0.3}$, $PM_{0.5}$ and $PM_{3.0}$). The particles concentration in the upstream (ambient air of a clean room) was calibrated before each measurement (no textile placed on the isokinetic probe of the apparatus).

The pressure drop (ΔP, Pa) of a filter was measured from the difference between the upstream and downstream pressures under air flow of 11.5 mL/min according to the following equation:

$$\Delta P = P_{upstream} - P_{downstream}$$

where $P_{downstream}$ and $P_{upstream}$ are the downstream and upstream pressures, respectively.

2.2.4. ADBAC loading on textiles

Functionalized textiles were impregnated in ADBAC aqueous solutions (PP-CD-0.2%, PP-CD-0.5% and PP-CD-1.0%). In order to evaluate the fastness of ADBAC, textiles were washed 1, 2, and 3 times for 1 minute in distilled water. Textiles disks were cut off with a punch in 11 mm-diameter disks and placed into a 24 well plate containing 1 mL of 0.15 M sodium hydroxide solution (Sigma Aldrich, France) during 4 hours at 37 °C under shaking (80 rpm). This treatment led to a complete hydrolysis of the cyclodextrin polymer coating and the total release of ADBAC from the samples in the supernatant. The supernatant solution was filtered (0.45 µm) and analyzed by Ultra-High-Performance Liquid Chromatography (UHPLC) coupled to DAD detection (UHPLC-DAD) (Nexera i, Shimadzu, Japan). The analyzed solutions containing ADBAC were separated with a reverse-phase column (C18 Diphenyl SpeedCore 2.6 µm, 100 × 2.1 mm, Fortis, England) maintained at 30 °C. The mobile phase consisted of acetonitrile/0.1M ammonium acetate, 0.2% phosphoric acid (65:35). The flow-rate was 0.3 mL/min and the injection volume 50 µL. Two peaks of ADBAC around 3.9 min and 5 min were detected at 214 nm. Both peaks areas were added to determine the total amount of ADBAC released.

2.2.5. Antibacterial efficacy

Kill-time test was performed to evaluate the kinetics of the bacterial reduction to determine the antibacterial activity of textiles samples against *S. aureus* (ATCC8739). Textiles samples (11 mm diameter disks) were placed into 24 well plates (CytoOne®). Then, 200 µL of a bacterial suspension (approximatively 1×10^7 CFU/mL) were placed on the textile samples and the plate was incubated at 37 °C. At each interval time the samples were removed from the well and placed in 2 mL of phosphate buffer saline (PBS, pH 7.4), treated in an ultrasonic bath for 1 min and vortexed for 30 s to collect the living bacteria. Successive 1/10 dilutions in cysteinated Ringer solution (CR) were made up to 10−4 from the recovered bacterial suspension and 0.1 mL of each dilution was seeded onto Mueller-Hinton agar (MHA). The plates were then incubated for 24 h at 37 °C. The number of viable bacteria was counted and expressed in Log CFU/mL.

2.2.6. Antiviral evaluation

Intrinsic antiviral activity of ADBAC

The virucidal assays were performed using human Coronavirus strain 229E (HCoV-229E). ADBAC solution (0.002%, 0.02%, and 0.2%) was added to a virus test suspension in a solution of interfering substance (Bovine Serum Albumin (BSA), 0.3 g/L). The mixture was maintained at 37 °C for 1 minute, 5 minutes, and 20 minutes. An aliquot was taken at the end of these contact times; the virucidal activity was immediately quenched using a validated method (MicroSpinTM S400 HR column filtration and dilution in ice-cold cell storage medium). The dilutions were transferred to cell cultures (Huh-7 cells), DMEM + glutamax supplemented with 10 % SVF and 1 % antibiotics). HuH-7 cell line, isolated from human liver[40], was obtained from Molecular and Cellular Virology of Coronavirus team, Center for Infection and Immunity of Lille, France. These cells were themselves sensitive to ADBAC, meaning that for the higher concentration 0.2%, a cytotoxic effect was observed on cells up to a 10^{-1} dilution of the suspension, that did not allow the virus to infect them; for larger dilutions (10^{-2} and beyond), this effect was lifted. After incubation, the infectious titers were calculated according to the method of Spearman[41] applied in standard NF EN 14476. The cytotoxic effect of ADBAC means that the detection limit was 2.5 log $TCID_{50}$/mL for 0.2% ADBAC, while it was 1.5 log $TCID_{50}$/mL for 0.02% and 0.002% ADBAC. The reduction in virus infectivity was calculated and corresponded to the difference in the titers of the virus, expressed in log, before (viral control) and after treatment with the product. The

analysis was carried out with an adaptation of the test method from standard NF EN 14476+A2 (2019): for practical reasons, the volumes used for the tests were reduced but retained the proportions described in the standard.

Antiviral activity of textiles loaded with ADBAC

The tests were carried out according to the requirements and specifications of ISO 18184 (2019) with minor adaptations (modification of the neutralizer and the volume of recovery). A virus test suspension was prepared at a known concentration. 200 µL of the suspension of test were deposited in micro-droplets (5 µL) on 0.4 g of pieces of textile of 2 cm x 2 cm (20 pieces). Textiles (treated and untreated) were kept at 20 °C for 5 minutes, 20 minutes, 1 hour, 2 hours, and 4 hours. At the end of the contact times, the textiles were immersed in 10 mL of neutralizer to immediately stop the action of the active substance. The number of surviving viruses was determined quantitatively by Spearman and Kärber's method. The results in TCID50/mL in the neutralizer were multiplied by ten to have the viral load on textiles.

3. Results and discussion

3.1. Chemicals process parameters for MS50 finishing with cyclodextrin

The process of textile finishing is based on the reaction between cyclodextrin and a polycarboxylic acid that react under curing conditions through esterification leading to the formation of a crosslinked CD polymer coating on the fibers[32]. In the present study preliminary tests on polypropylene MS50 filter displayed slight shrinking under curing (sample dimensions reduced in the range of 5%) from 130°C. Therefore, the low thermal stability of the PP filter limited the curing temperature to 130°C. As crosslinking reaction rate evolves conversely with curing temperature, the first challenge tackled here was to immobilize cyclodextrin by curing treatment at limit temperature of 130°C within the shortest possible time in compliance with the targeted process industrial upscaling. Based on our previous results, a comparative study displayed that the lowest threshold curing temperature for provoking esterification between citric acid and different cyclodextrins derivates were obtained for HPβCD compared with γCD, βCD and αCD respectively. So, in presence of HPβCD it was possible to treat polypropylene and PLLA inguinal meshes for hernia repair under curing temperature of 140°C during 30 minutes and 60 minutes respectively with a reactant mixture containing HPβCD and citric acid (CTR) without damaging the textiles[34,35]. The choice of the polycarboxylic acid is also important. In a previous study, we reported that the reactivity of polycarboxylic acids may also differ, and we reported that 1,2,3,4-butanetetracarboxylic acid (BTCA) presented higher reactivity than CTR and drastically lowered the threshold temperature of curing[32]. The third component of the reactive solution is the phosphorous salt used as esterification catalyst. The process was initially developed using sodium mono- and dihydrogen phosphate and sodium dihydrogen hypophosphite[32]. In the present study, ammonium hypophosphite was compared with sodium hypophosphite in order to investigate the effect of the counterion of hypophosphite (ammonium *vs* sodium) on the catalyst efficiency.

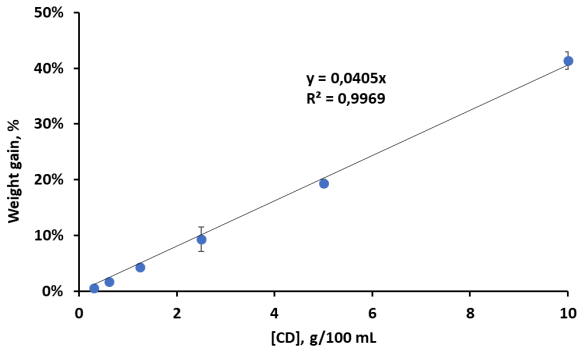

So, based on our previous studies mentioned above, MS50 filters were treated with HPβCD, BTCA and CTR as crosslinking agents, and $NH_4H_2PO_2$ and NaH_2PO_2 as catalysts. With the objective of optimizing the process, a non-ionic surfactant (Erkantol®) was also added in the padded solutions in order to increase the wet pick-up of MS50 made of hydrophobic PP fibers. Fig 1A displays the evolution of the weight gain of samples versus time at 120°C, 125°C and 130°C treated with CTR and BTCA (catalyst, $NH_4H_2PO_2$). CTR displayed threshold reaction time of 10 min at 130 °C and of 15 min at lower temperatures. Besides, in presence of BTCA, weight gain increased from only 150 sec at 130°C and the maximal values are reached after 5 min of curing at the three investigated temperatures. Fig 1B displays the evolution of the weight gain of samples versus time of curing at 120°C, 125°C and 130°C, treated with BTCA and catalysed by NaH_2PO_2 and $NH_4H_2PO_2$. The use of $NH_4H_2PO_2$ displayed significant threshold reductions of curing time and curing temperature compared to NaH_2PO_2. As a matter of fact, in presence of the ammonium salt, significative amounts of cyclodextrin polymer were observed on samples treated during 2.5 minutes at 125°C (18.8%) and 130°C (31,4%), while less than 5.8% weight gains were measured in presence of the sodium salt at these temperatures. Interestingly, a weight gain of 34.4% was reached within 5.0 minutes at 120°C. So, the combination of BTCA and ammonium hypophosphite drastically lowered the time and the curing temperature for coating the MS50 filter with the cyclodextrin polymer so that the standard curing parameters applied in the

following of the study were temperature of 125°C during 5 minutes.

Figure 1 – Influence of the curing time and curing temperature (■ 120°C, ● 125°C, ◆ 130°C) on the weight gain of the nonwoven PP after functionalization. A) using BTCA as crosslinking agent (BTCA/$NH_4H_2PO_2$/HPβCD/Erkantol®

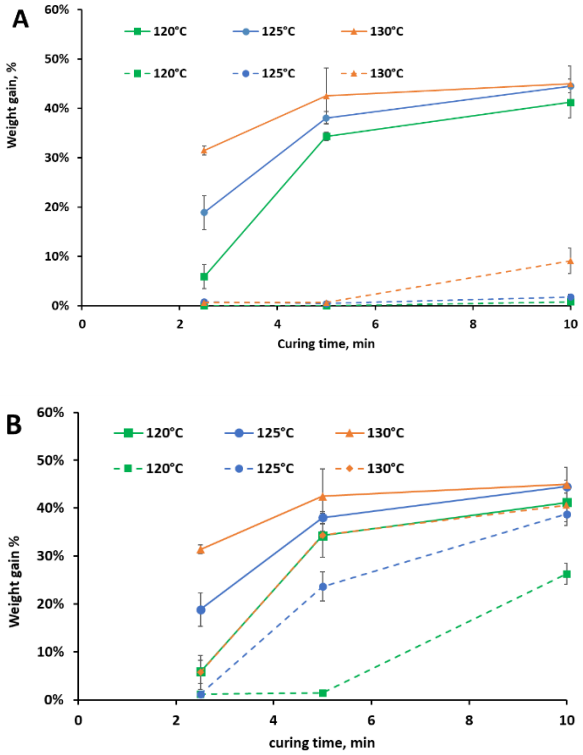

(Formulation 10/3/10/1 in g/100mL, solid line)) and using citric acid as crosslinking agent (CTR/$NH_4H_2PO_2$/HPβCD/Erkantol® (Formulation 10/3/10/1 in g/100mL, dotted line)). B) using BTCA as crosslinking agent and ammonium hypophosphite as catalyst

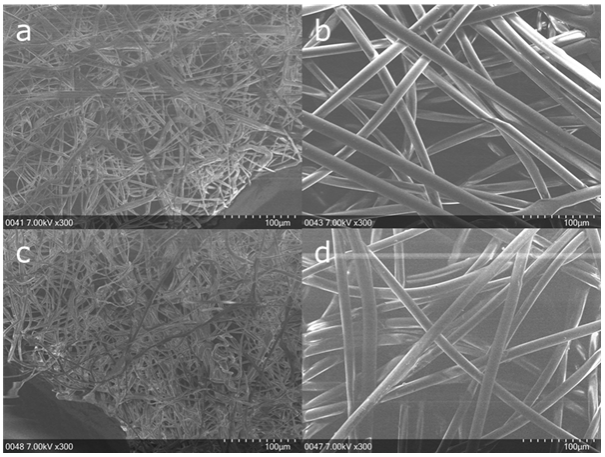

(BTCA/$NH_4H_2PO_2$/HPβCD/Erkantol® (Formulation 10/3/10/1 in g/100mL, solid line)) and sodium hypophosphite as catalyst (BTCA/NaH_2PO_2/HPβCD/Erkantol® (Formulation 10/3/10/1 in g/100mL, dotted line)), n=3.

Samples were then treated with different dilutions of the mother solution BTCA/$NH_4H_2PO_2$/HPβCD corresponding to weight ratio 10g/3g/10g for 100 mL of water, keeping constant surfactant concentration at 1%$_{v/v}$ in all solutions. As observed in Figure 2, a linear relation between the concentration of the padding solution and weight gain of MS50 measured after pad/dry/cure process, hand washing and drying was observed.

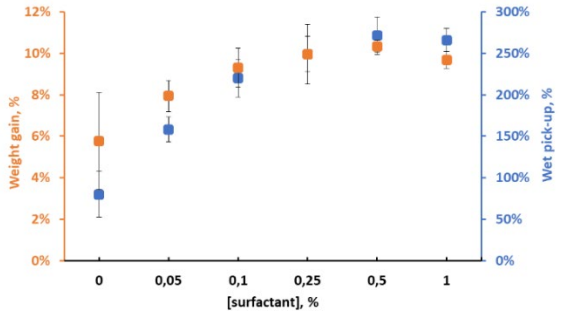

These results allowed to define the concentration of the padding solution BTCA / $NH_4H_2PO_2$ / HPβCD / surfactant mixture with ratio 2.5/0.5/2.5/1 for a targeted final weight gain of 10% due to BTCA-HPβCD polymer immobilization.

Figure 2: Weight gain of nonwoven PP padded with different dilutions (C, C/2, C/4, C/8, C/16, C/32). Mother solution (C) formulation was BTCA / $NH_4H_2PO_2$ / HPβCD (Formulation 10/3/10 expressed in g/100mL) and 1%$_{v/v}$ or Erkantol® in all solutions. Samples were cured at 125 °C during 5 minutes, washed and dried before weight gain measurement. n=3.

The influence of the surfactant concentration in the padded solution was investigated. Figure 3 reports the wet pick-up increase from 130% up to 240% upon gradually increasing Erkantol® concentration up to 1%$_{v/v}$. As a consequence, the parallel increase of the final weight gain after curing was observed, from 3% up to 10%. The maximal value of weight gain was reached with a 0.5%$_{v/v}$ concentration of surfactant, however, in order to avoid bath exhaustion, the surfactant concentration was fixed at 1%$_{v/v}$. So, the use of the surfactant clearly enhanced the yield of the pad/dry/cure process of functionalization by promoting the aqueous reactants solution absorption by the hydrophobic polypropylene fibers. To summarize the process parameters study, the standard formulation adopted was BTCA/$NH_4H_2PO_2$/HPβCD/Erkantol® (2.5 / 0.5 / 2.5 / 1) and curing at 125 °C during 5 minutes.

Figure 3: Influence of surfactant concentration (Erkantol®) on the wet pick-up after padding step (blue line) and on the final weight gain (red line) of the nonwoven PP after curing at 125°C during 5 minutes, washing and drying steps. The formulation of the impregnating solution was BTCA/$NH_4H_2PO_2$/HPβCD /Erkantol® (Formulation: 2.5/0.5/2.5/X expressed in g/100mL), n=3.

3.2.SEM observation

Figure 4: SEM micrographs of Meltblown side of non-woven PP before (a) and after (c) finishing treatment. Spunbond side before (b) and after (d) finishing treatment. The solution was BTCA / $NH_4H_2PO_2$ / HPβCD / Erkantol® (Formulation 2.5 / 0.5 / 2.5 / 1, expressed in g for 100mL). The finishing curing parameters were 125°C, 5 minutes

As observed in figure 4, micrographs of both faces of MS50 display no visible difference before and after finishing treatment in standard conditions defined above. Meltblown fibers present diameter in the range of 2-3 µm against 15-20 µm for spunbond fibers. Despite functionalization in the standard conditions yielding a weight gain value of 10%, SEM photos could neither evidence cyclodextrin polymer coating on fibers, nor the formation of clogs in the entangled PP filaments network. Thus, CD polymer is homogeneously spread on the nonwoven material without modifying the porosity of the MS50 filter.

3.3.Filtration efficiency and air permeability

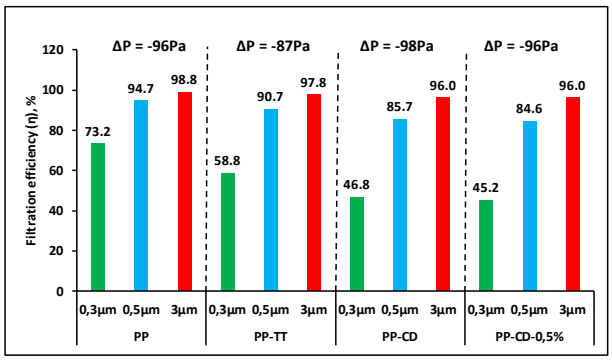

Figure 5: Pressure drops (ΔP) and filtration efficiency toward particles of diameter 0.3, 0.5 and 3.0 µm for textiles: raw PP, PP with thermal treatment at 125°C during 5 minutes (PP-TT), PP-CD (PP-CD, weight gain = 10%), PP-CD impregnated with ADBAC 0.5% (PP-CD-0.5%).

Figure 5 reveals a slight decrease of the filtration efficiency from 98.8 % down to 96.0 % toward particulate matter of 3 µm ($PM_{3.0}$) and from 94.7% down to 85.7% toward 0.5 µm particles ($PM_{0.5}$) when comparing raw PP and PP-CD. A larger difference was observed in the case of 0.3 µm particles ($PM_{0.3}$) with values decreasing from 73.2% down to 46.8%. It is noteworthy that after padding in water and heat treatment at 125 °C during 5 minutes (blank treatment), PP-TT sample also displayed a sharp decrease of filtration efficiency toward $PM_{0.3}$ down to 58.8%. Particulate matter capture on filters occur by gravity sedimentation, interception, inertial impaction, diffusion, and electrostatic attraction[42]. The filters which combine the inertial, interception, and diffusion mechanisms are known as mechanical filters. The charged filters displaying electrostatic attraction are so-called "electrets filters" in the literature[43]. The electrostatic phenomena are especially involved in the capture of the thinnest particles. As a consequence, the more extended decrease of filtration efficiency toward the thinnest particles $PM_{0.3}$ compared with $PM_{3.0}$ and $PM_{0.5}$ can be attributed to the loss of electrostatic charge upon the textile finishing process. Interestingly, as also observed in Figure 5, the values of ΔP and filtration efficiency toward the three categories of particulate matters did not change after impregnation of PP-CD in the ADBAC solution.

Unlike filtration efficiency, pressure drop values reported in figure 5 values were not markedly affected after cyclodextrin treatment nor after blank treatment (ΔP was almost kept constant in the range of -96 Pa). This result agrees with the microscopy study which did not evidence any degradation of the nonwoven porosity upon treatment.

3.4.ADBAC loading

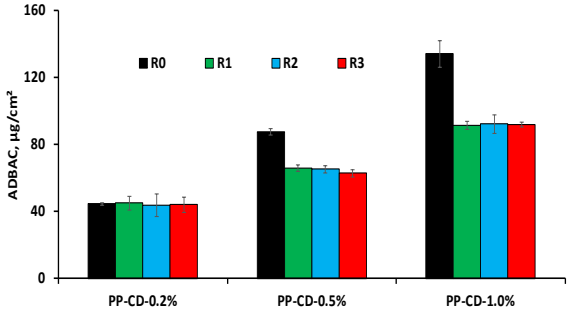

Figure 6: ADBAC (in µg/cm²) loaded on PP-CD samples after impregnation in ADBAC solutions of concentrations 0.2%$_{w/v}$, 0.5%$_{w/v}$ and 1.0%$_{w/v}$, (respectively PP-CD-0.2%, PP-CD-0.5% and PP-CD—1.0% after impregnation (R0), and after each of 3 successive rinsing in distilled water during 1 minute (R1, R2, R3)

PP-CD samples were impregnated in ADBAC solutions of variable concentrations for their antimicrobial activation. The adsorbed ADBAC expressed in µg/cm² was determined after impregnation and drying (R0) and after each of the three successive rinsing / drying steps applied (R1 to R3). The quantities of adsorbed ADBAC on PP-CD samples increased with ADBAC concentration in solution from 44 µg/cm² (PP-CD-0.2%) up to 134 µg/cm² (PP-CD-1%). Interestingly, no ADBAC leaching was detected at the first rinsing for PP-CD-0.2%. Besides, leakage of 26% (21.6 µg/cm²) and 31% (42.5 µg/cm²) of loaded ADBAC was observed from the first rinsing for samples impregnated in 0.5% and 1.0% ADBAC solutions, respectively, and no ADBAC was then released in the second and third rinsing for all tested samples. These result evidence dual interaction of ADBAC with PP-CD. Firstly, there is a fraction of ADBAC easily removed by the rinsing which can be called "excess" ADBAC. Secondly, there is an ADBAC fraction that resists to the rinsing, which is bound to the fibers by stronger interactions. On the one hand the "excess" ADBAC is physically adsorbed on the textile through physical (van der Waals) interactions, and on the other hand, "bound" ADBAC interacts with the cyclodextrin polymer coating. Two types of interactions involved in the latter case are i) inclusion complexation of ADBAC in the cyclodextrin cavities and ii) ionic interactions between the cationic quaternary ammonium group of ADBAC and the anionic carboxylate group of the citrate crosslinks of the cyclodextrin polymer. Indeed, we already reported such dual interaction mechanisms in case of a Dacron® based vascular prosthesis modified by the same process of cyclodextrin functionalization for the sorption of ciprofloxacin, an amphoteric molecule, and of methylene blue, a cationic dye[44,30]. Interestingly, a proton NMR study in solution with ROESY sequence evidenced the complexation of ADBAC in the cavities of native and polymerized forms of βCD by inclusion of C12-C16 alkyl chains rather than by inclusion of the phenyl group [see Figure S1, supplementary data].

3.5.Kill time tests

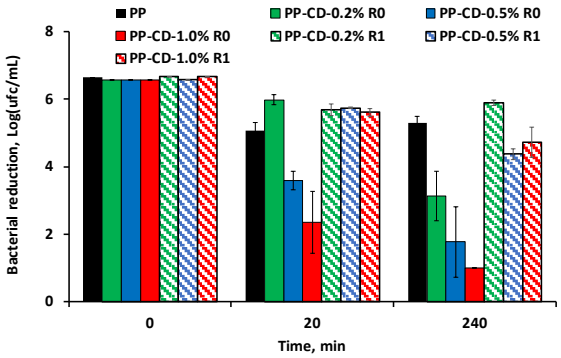

Figure 7: Kinetic of bacterial reduction of S. aureus in contact with PP-CD impregnated with 0.2%, 0.5% and 1.0% ADBAC solutions (respectively PP-CD-0.2%, PP-CD-0.5% and PP-CD-1.0%, without rinsing (R0) and after rinsing step (R1), n=3.

Figure 7 shows that the antibacterial activity of PP-CD *against S. aureus* increased with the concentration of the ADBAC solution after the impregnation (R0) and after the first rinsing (R1). Concerning untreated PP control, a 1.2 log_{10} decrease is observe after 20 and 240 minutes of contact. This decrease can be explained by the natural mortality of bacteria in contact with a hydrophobic rough textile, as we recently observed in another study on the functionalization of a non-woven polypropylene with antibacterial polyvinyl alcohol-based nanofibers[45] (Oderich Muniz et al., 2022). After 20 minutes of contact, the antibacterial activity of PP-CD-0.2%, PP-CD-0.5% and PP-CD-1% increased with ADBAC concentration from -0.6 log_{10} to -3.0 log_{10} and up to -4.2 log_{10}. After 4 hours of contact, the PP-CD-0.2% sample reached a relevant antibacterial activity of -3.4 log_{10}. After rinsing (R1), a sharp decrease of the antimicrobial performance of samples was observed as bacterial reduction was only -1 log_{10} after 20 minutes and -2 log_{10} after 4 hours for PP-CD-0.2% R1, PP-CD-0.5% R1 and PP-CD-1% R1, respectively. Two conclusions can be deduced from these results: in order to reach a fast and efficient antibacterial effect, 1) samples should be activated with ADBAC solution of minimum concentration of 0.2%, and 2) samples should not be rinsed after the ADBAC impregnation step so that “bound” and “excess” ADBAC are present on the textile filter. The “excess” ADBAC presents fast killing of bacteria because it is bioavailable. On contrary, the bound ADBAC has low antibacterial activity due to interactions of the quaternary ammonium groups with carboxylic acid groups of the polyBTCA-CD polymer, and inclusion of the C12-C18 alkyl chains in CD cavities.

The toxicity of ADBAC is an important point to consider, especially in the case of not rinsed samples that could release the “excess” ADBAC in the damp air flow of breath, passing through the filtering layers of the mask and reach the respiratory system. In a rat model, the *no observed adverse effect level* (NOAEL) for adult and offspring systemic toxicity is 59 mg/kg/day. The NOAEL for maternal toxicity was 1 mg/kg/day and the NOAEL for prenatal developmental toxicity was 20 mg/kg/day [46,47]. According to standard on Barrier masks - Guide to minimum requirements, test methods, manufacture and use (AFNOR -SPEC S76-00), the maximum surface of a mask is 194.5 cm². Figure 6 shows that for PP-CD-1.0%, the total amount of ADBAC is 134.0 µg/cm² with a free amount of 42.0µg/cm² (in the worst case – total immersion of the functionalized layer in the water, no barrier layers like in a full-face mask). Thus, for a person weighing 60 kg on average, the maximum doses would be 0.14 mg/kg/day if all the ADBAC was released. Even though we are in the worst condition, the dose is well below the NOAEL.

3.6.Antiviral activity

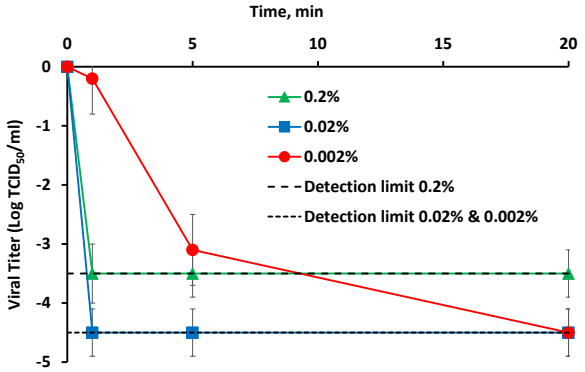

Figure 8: Virucidal activity of ADBAC solutions concentrated at 0.002, 0.02 and 0.2 %w/v in contact with HCoV-229E during 1, 5 and 20 minutes.

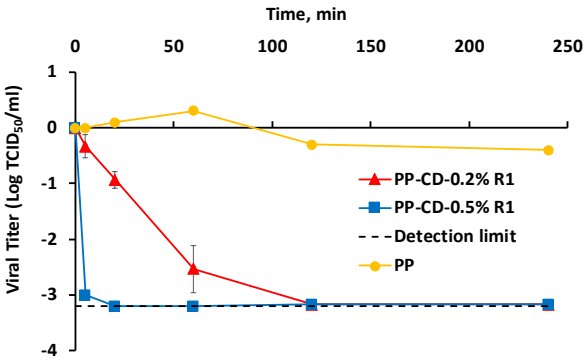

Figure 9: Virucidal activity of PP and PP-CD sample impregnated in ADBAC solutions (0.2% and 0.5%) after one rinsing step (R1)

According to the methodology adapted from standard NF EN 14476 + A2 (July 2019) under clean conditions, ADBAC has a virucidal activity with respect to the strain of human Coronavirus 229E greater than or equal to 4.5 log at the test concentration of 0.02% for a contact time of 1 minute, and at the test concentration of 0.002% for a contact time of 20 minutes (Figure 8). For ADBAC at 0.2%, a virucidal activity greater than or equal to 3.5 log was observed after a contact time of 1 minute; the detection limit is higher at this concentration because of the toxicity of ADBAC on Huh-7 cells used to count the virus. Detection limits are indeed based on both the initial viral concentration and the toxicity level of the product on cells. Therefore, reductions are given as 'greater

than or equal to' some value, but the actual (possibly quite larger) reduction is unknown.

PP, PP-CD0.5% R1 and PP-CD-0.2% R1 were tested on HCoV-229E strain in direct contact. According to the protocol of standard ISO 18184, PP does not show antiviral activity whereas PP-CD-0.2% R1 exhibits antiviral activity on the human coronavirus strain 229E from 0.9 log i.e. 87.9% reduction in viral load after 20 minutes, 2.5 log i.e. 99.7% reduction in viral load after 1 hour and more than 3.2 log, i.e. a reduction in viral load of more than 99.94% after 2 hours. In the same way, PP-CD-0.5% R1 exhibits antiviral activity on the human coronavirus strain from 3.0 log i.e. 99.9% reduction in viral load after 5 minutes, and more than 3.4 log, i.e. a reduction in viral load of more than 99.96% after 20 min (Figure 9). Two conclusions can be deduced from these results 1) ADBAC present a rapid and important antiviral activity in solution (0.02%v/v) 2) Rinsed samples presents fast deactivation of virus (99.96% in 20 min) despite the rinsing step. In contrast with antibacterial test, bound ADBAC has a very important virucidal activity.

This difference can be explained by 1) the mechanism of action of ADBAC on bacteria and viruses. Viruses, especially enveloped viruses such as coronaviruses, are more sensitive to adverse environment[48,49]. Their membrane is easier to damage than other microbial structures. Furthermore, other parts of the virus (especially RNA) may be damaged by ADBAC[50], thus leading to an increased sensitivity compared to bacteria. 2) The size of the microorganisms. While viruses are a few nanometres in size, bacteria are in the micrometre range. This size difference could explain the need for free ADBAC to eliminate bacteria while smaller viruses are in contact more easily with fixed ADBAC and can be fixed on a surface. 3) The textile-to-strain ratio is different in antibacterial test and in the antiviral test. While 200 µL of bacterial suspension are deposited on a 11 mm diameter disc, 200 µL of viral suspension are deposited on 133 cm² of textile in 5 µL droplets. The interaction between virus and textile is closer those with bacteria.

4. Conclusion

The functionalization of MS50 by a cyclodextrin polymer was optimized in term of curing parameters, reaction kinetic and reaction yield by the systematic investigation of the padded solution. The formulation based on HPβCD/ammonium hypophosphite/BTCA/surfactant of weight ratio 2.5/0.5/2.5/1 resulted in successful results under low curing temperature of 125°C within the short curing time (5 minutes) that preserved the filter structure and its breathability. Samples were then activated by padding in ADBAC solutions. Antibacterial tests on *S. aureus* revealed that "excess" ADBAC adsorbed by weak interactions on the modified textile was necessary for providing significant bacterial reduction. Such activity drastically decreased after removal of the "excess" ADBAC after one rinsing. Besides, virucidal tests realized on rinsed samples displayed significant activity (99.96% reduction within 20 minutes). MS50-CD-ADBAC samples are intended for surgical and FFP2 or N95 masks manufacture where they will be inserted as the inner self-decontaminating layer in the multilayer assembly of the masks. In this way, the active layer will not be directly in contact with face. The face side layer will play the role of barrier preventing ADBAC migration toward both sides of the mask. The next part of the study will aim to evaluate the effectiveness of the facepiece respirators in terms of filtration, breathability, and safety with assessment of eventual migration of ADBAC through the layers of the mask finally we will investigate the biocide effectiveness of the masks against airborne viruses in air flow conditions.

Author Contributions

We strongly encourage authors to include author contributions and recommend using CRediT for standardised contribution descriptions. Please refer to our general author guidelines for more information about authorship.

- **Mickael Maton**: Investigation, methodology
- **Sarah Gabut**: Investigation
- **Christel Neut** : Validation, methodology, Writing – review & editing
- **Pascal Odou**: Investigation, methodology, validation, Writing – review & editing
- **Camille Sacareau**: investigation, methodology
- **Anthony Pinon**: Supervision, validation, Writing – review & editing
- **Michèle Vialette**: Supervision, validation
- **Gaétan Gerber**: Resource, funding acquisition, visualisation, project adminitration
- **Bernard Martel**: Conceptualization, supervision, funding acquisition, validation, visualization, writing original draft, project administration, Writing – review & editing
- **Nicolas Blanchemain**: Conceptualization, supervision; funding acquisition, validation, visualization, writing original draft, project administration, Writing – review & editing

Conflicts of interest

There are no conflicts to declare

Notes and references

1. V.C.C Cheng, S.C. Wong, V.W.M. Chuang, S.Y.C. So, H.H.K. Chen, S. Sridhar, K.K.W. To, J.F.W. Chan, I.F.N. Hung, P.L. Ho, K.Y. Yuen. *Journal of Infection*, 2020, **81**, 107–114
2. A.A. Chughtai, S. Stelzer-Braid, W. Rawlinson, G. Pontivivo, Q. Wang, Y. Pan, D. Zhang, Y. Zhang, L. Li. MacIntyre, C.R. *BMC Infectious Diseases,* 2020, **19**, 491
3. S.J. Chang, Y.C. Chang, K.Z. Lu, Y.Y. Tsou, C.W. Lin. *Evid Based Complement Alternat Med,* 2012, 925830–925830
4. V. Babaahmadi, H. Amid, M. Naeimirad, S. Ramakrishna. *Science of The Total Environment*, 2021, **798**, 149233
5. I. Cerkez, S.S. Worley, R.M. Broughton, T.S. Huang. Reactive and Functional Polymers, 2013, **73**, 1412–1419.
6. J. Huang, H. Murata, R.R. Koepsel, A.J. Russell, K. Matyjaszewski. Biomacromolecules, 2007, **8**, 1396–1399.
7. E.S. Abdou, S.S. Elkholy, M.Z. Elsabee, E. Mohamed. *Journal of Applied Polymer Science*, 2008, **108**, 2290–2296.
8. C. Radheshkumar, H. Münstedt. *Reactive and Functional Polymers*, 2006, **66**, 780–788.

9. I. Torres, B. Gonzalez-Tobío, P. Ares, J. Gomez-Herrero, F. Zamora. Materials Today Chemistry. 2022, 26, 101146.
10. C. Balagna, S. Perero, E. Percivalle, E. V. Nepita, M. Ferraris. Open Ceramics. 2020, **1**, 100006.
11. I. Cerkez, H.B. Kocer, S.D. Worley, R.M. Broughton, T.S. Huang. N-Halamine. *Langmuir*, 2011, **27**, 4091–4097.
12. N. Sanbhal, Y. Mao, G. Sun, R.F. Xu, D. Zhang, L. Wang. *Applied Surface Science*, 2018, **439**, 749–759
13. M. Sorci, T.D. Fink, V. Sharma, S. Singh, R. Chen, B. Arduini, K. Dovidenko, C. L. Heldt, E. F. Palermo, R.H. Zha. *ACS Appl. Mater. Interfaces* 2022, 14, 25135−25146.
14. S. Kumaran, E. Oh, S. Han, H-J. Choi. Photopolymerizable. Nano Lett. 2021, **21**, 5422−5429
15. D.L. Lovell. Zephiran. *Archives of Surgery*, 1946, **53**, 304–311
16. P.B. Price. *Archives of Surgery*, 1950, **61**, 23–33.
17. B. Merchel Piovesan Pereira, I. Tagkopoulos. *Appl Environ Microbiol*, 2019, **85**, e00377-19.
18. A. Luz, P. DeLeo, N. Pechacek, M. Freemantle? Regulatory Toxicology and Pharmacology. 2020, **116**,104717
19. R. Dolezal, O. Soukup, D. Malinak, R.M.L. Savedra, J. Marek, M. Dolezalova, M. Pasdiorova, S. Salajkova, J. Korabecny, J. Honegr, T.C. Ramalho, K. Kuca. *European Journal of Medicinal Chemistry*, 2016, **121**, 699–711.
20. J.H. Kang, J.B. Park, K.B. Song. *LWT*, 2019, **102**, 284–290.
21. A. Badura, J. Krysiński, A. Nowaczyk, A. Buciński. *Arabian Journal of Chemistry*, 2021, **14**, 103233.
22. B.H. Ogilvie, A. Solis-Leal, J.B. Lopez, B.D. Poole, R.A. Robison, B.K. Berges. *Journal of Hospital Infection*, 2021, **108**, 142–145.
23. H.F. Rabenau, G. Kampf, J. Cinatl, H.W. Doerr. *Journal of Hospital Infection*, 2005, **61**, 107–111.
24. G. Dev Kumar, S. Ravishankar, V.K. Juneja. *in: Juneja, V.K., Dwivedi, H.P., Sofos, J.N. (Eds.), Springer New York, New York, NY*, 2017, pp. 199–223.
25. E. Smolková-Keulemansová. Cyclodextrins and their inclusion complexes: by J. Szejtli, Akadémiai Kiadó, Budapest, 1982, 296 pp
26. E. Jean-Baptiste, N. Blanchemain, C. Neut, F. Chai, M. Maton, B. Martel, H.F. Hildebrand, S. Haulon. *Journal of Infection*, 2014, **68**, 116–124.
27. A. Mogrovejo-Valdivia, O. Rahmouni, N. Tabary, M. Maton, C. Neut, B. Martel, N. Blanchemain. *International Journal of Pharmaceutics,* 2019, **556**, 301–310
28. N. Tabary, F. Chai, N. Blanchemain, C. Neut, L. Pauchet, S. Bertini, E. Delcourt-Debruyne, H.F., Hildebrand, B. Martel. *Acta Biomaterialia*, 2014, **10**, 318–329.
29. S. Ouerghemmi, S. Degoutin, N. Tabary, F. Cazaux, M. Maton, V. Gaucher, L. Janus, C. Neut, F. Chai, N. Blanchemain, B. Martel. *International Journal of Pharmaceutics*, 2016, **513**, 483–495.
30. I. Kacem, T. Laurent, N. Blanchemain, C. Neut, F. Chai, S. Haulon, H.F. Hildebrand, B. Martel. *Journal of Biomedical Materials Research Part A*, 2014, **102**, 2942–2951.
31. T. Loftsson, K. Matthíasson, M. Másson. *International Journal of Pharmaceutics*, 2003, **262**, 101–107.
32. B. Martel, M. Weltrowski, D. Ruffin, M. Morcellet. *Journal of Applied Polymer Science*, 2002, **83**, 1449–1456.
33. Y. El Ghoul, N. Blanchemain, T. Laurent, C. Campagne, A. El Achari, S. Roudesli, M. Morcellet, B. Martel, H.F. Hildebrand. *Acta Biomaterialia*, 2008, **4**, 1392–1400.
34. G. Vermet, S. Degoutin, F. Chai, M. Maton, C. Flores C. Neut, P.E. Danjou, B. Martel, N. Blanchemain. *Acta Biomaterialia*, 2017, **53**, 222–232.
35. T. Laurent, I. Kacem, N. Blanchemain, F. Cazaux, C. Neut, H.F. Hildebrand, B. Martel. *Acta Biomaterialia*, 2011, **7**, 3141–3149.
36. M. Frouin, B. Martel, N. Blanchemain. 2022, WO2022/162139 A2.
37. S. Skorupinski, A. Baillie, H. Dordhain, N. Blanchemain, B. Martel, G. Rawel, F. Durand, B. Letartre, J. Criquelion.. 2013, FR 2984176
38. L. Ducoroy, M. Bacquet, B. Martel, M. Morcellet.. *Reactive and Functional Polymers*, 2008, **68**, 594–600.
39. A. Tcharkhtchi, N. Abbasnezhad, M. Zarbini Seydani, N. Zirak, S. Farzaneh, M. Shirinbayan. *Bioactive Materials*, 2021, **6**, 106–122.
40. H. Nakabayashi, K. Taketa, K. Miyano, T. Yamane, J. Sato. *Cancer Research*, 1982, **42**, 3858 –3863. PMID: 6286115
41. C. Spearman. *British Journal of Psychology*, 1908, 227–242
42. H. C. Yeh and B. Y. H. Liu. *J. Aerosol*, 1974, **66,** 191–204
43. E. Tian, Y. Gao, J. Mo. Building and Environment, 2023, **228**, 109782
44. N. Blanchemain, Y. Karrout, N. Tabary, M. Bria, C. Neut, H.F. Hildebrand, J. Siepmann, B. Martel. *Carbohydrate Polymers*, 2012, **90**, 1695–1703.
45. N. Oderich Muniz, S. Gabut, M. Maton, P. Odou, M. Vialette, A. Pinon, C. Neut, N. Tabary, N. Blanchemain, B. Martel. Nanomaterials, 2023, **13**, 9
46. K.A. Hostetler, L.C. Fisher, B.L. Burruss. *Birth Defects Research*, 2021b, **113**, 1368–1389.
47. K.A. Hostetler, L.C. Fisher, B.L. Burruss. *Birth Defects Research*, 2021a, **113**, 925–944.
48. G. McDonnell, AD. Russell. Clin Microbiol Rev., 1999, 12(1):147-79.
49. S. Firquet, S. Beaujard, PE. Lobert, F. Sané, D. Caloone, D. Izard, D. Hober. Microbes Environ. 2015;30(2):140-4.
50. A.G. Caschera, J. McAuley, Y. Kim, D. Purcell, J. Rymenants, D.A. Foucher. American Journal of Infection Control, 2022, **50**, 325−329.